Title
Liquid-liquid phase separation in aerosol particles: imaging at the nanometer scale.

Journal
Environmental science & technology, 49(8)

ISSN
0013-936X

Authors
O'Brien, Rachel E
Wang, Bingbing
Kelly, Stephen T
et al.

Publication Date
2015-04-01

DOI
10.1021/acs.est.5b00062

Peer reviewed

Environmental Science & Technology

Article

pubs.acs.org/est

Liquid–Liquid Phase Separation in Aerosol Particles: Imaging at the Nanometer Scale

Rachel E. O'Brien,[†,#] Bingbing Wang,[‡] Stephen T. Kelly,[†,▽] Nils Lundt,[†,§,●] Yuan You,[⊥] Allan K. Bertram,[⊥] Stephen R. Leone,[†,§,∥] Alexander Laskin,[‡] and Mary K. Gilles*[,†]

[†]Chemical Sciences Division, Lawrence Berkeley National Laboratory, Berkeley, California 94720-8198, United States

[‡]William R. Wiley Environmental and Molecular Sciences Laboratory, Pacific Northwest National Laboratory, Richland, Washington 99352, United States

[§]Department of Chemistry, University of California, Berkeley, California 94720, United States

[∥]Department of Physics, University of California, Berkeley, California 94720, United States

[⊥]Department of Chemistry, University of British Columbia, Vancouver, British Columbia V6T 1Z1 Canada

Supporting Information

ABSTRACT: Atmospheric aerosols can undergo phase transitions including liquid–liquid phase separation (LLPS) while responding to changes in the ambient relative humidity (RH). Here, we report results of chemical imaging experiments using environmental scanning electron microscopy (ESEM) and scanning transmission X-ray microscopy (STXM) to investigate the LLPS of micrometer-sized particles undergoing a full hydration-dehydration cycle. Internally mixed particles composed of ammonium sulfate (AS) and either: limonene secondary organic carbon (LSOC), α, 4-dihydroxy-3-methoxybenzeneaceticacid (HMMA), or polyethylene glycol (PEG-400) were studied. Events of LLPS were observed for all samples with both techniques. Chemical imaging with STXM showed that both LSOC/AS and HMMA/AS particles were never homogeneously mixed for all measured RH's above the deliquescence point and that the majority of the organic component was located in the outer phase. The outer phase composition was estimated as 65:35 organic: inorganic in LSOC/AS and as 50:50 organic: inorganic for HMMA/AS. PEG-400/AS particles showed fully homogeneous mixtures at high RH and phase separated below 89–92% RH with an estimated 70:30% organic to inorganic mix in the outer phase. These two chemical imaging techniques are well suited for in situ analysis of the hygroscopic behavior, phase separation, and surface composition of collected ambient aerosol particles.

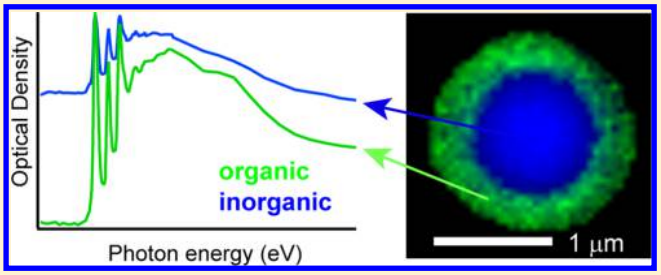

1. INTRODUCTION

Atmospheric particles containing both organic and inorganic components can undergo phase transitions such as deliquescence, efflorescence, and liquid–liquid phase separation (LLPS) responding to changes in the ambient relative humidity (RH).[1−3] Particles will have two separate phases when at least some fraction of the organic compounds are not miscible with the aqueous inorganic solution.[4] These phase separated particles can have either a core–shell or a partially engulfed morphology.[5,6] Particles with core–shell morphology with an organic shell can have suppressed water uptake and chemical reactivity with the aqueous core compared to partially engulfed particles which have the aqeuous inorganic phase in contact with the air.[7,8] Obtaining information on the morphology and the composition of the two phases is important for predictive understanding of aerosol effects on atmospheric environment and climate because they influence the gas/particle partitioning of semivolatile organic compounds,[9] rates of heterogeneous chemistry,[2] and the kinetics of water uptake.[10]

Recent work has been done analyzing LLPS in a variety of model systems. The dependence of LLPS on the oxygen to carbon ratios (O/C) of the organics[11] as well as the organic to inorganic ratio and the type of inorganic[12,13] indicated that LLPS events are common in mixed organic/inorganic aerosols in the troposphere. Using optical microscopy and/or Raman spectroscopy of relatively large particles (>10 um), both core–shell and partially engulfed morphologies have been observed.[2,5,14,15] In these studies, the outer coating was always the organic phase except when a hydrophilic substrate was used.[16] Recent work on these large particles has also demonstrated that LLPS can drive black carbon into the outer (organic) phase with potential impacts on the absorption enhancement of black carbon for particles containing all three components.[17] Experiments using cryo-TEM on dried organic/

Received: January 5, 2015
Revised: March 30, 2015
Accepted: March 31, 2015
Published: April 7, 2015

DOI: 10.1021/acs.est.5b00062
Environ. Sci. Technol. 2015, 49, 4995−5002

Table 1. RH Values Determined from ESEM Measurements for the Phase Changes (Deliquescence, DRH; Efflorescence, ERH; Liquid−liquid Phase Separation, SRH) in Organic/Ammonium Sulfate/Water Systems; All Values are ±2%

sample	DRH %	Lit.[b]	SRH%	Lit.	ERH%	Lit.
AS	82−84	~82[28]			31−34	~35[27]
LSOC/AS 2:1	75−78		90−92		35−37	
LSOC/AS 8:1	N/A[a]		92−94		30−32	
HMMA/AS 1:1	82−83		80−81	80[12]	31−34	
PEG 400/AS 1:1	83		90−91	89.5[14]	33−34	35[14]
PEG 400/AS 8:1	82−84	80[14]	89−92	88.7[14]	31−35	27[14]

[a]Deliquescence observed but DRH not measured. [b]Literature values, superscript citations.

ammonium sulfate particles have demonstrated a size dependence for phase separations. Veghte et al. found partially engulfed morphologies for particles larger than ~100−300 nm and homogeneous particles below this size cutoff.[18,19] A partially engulfed structure with inorganic on the outside was also observed for submicrometer particles of mixed adipic acid and ammonium sulfate.[20]

The resolution limits of optical microscopy and micro Raman spectroscopy preclude direct analysis of the phase behavior, morphology, and composition of impacted particles with diameters of approximately one micrometer and less, which is the size range of a majority of the particles in the atmosphere. Environmental scanning electron microscopy (ESEM) and scanning transmission X-ray microscopy with near edge X-ray absorption fine structure spectroscopy (STXM/NEXAFS) are spectromicroscopic techniques that provide images and chemical information on impacted aerosol particles at the nm and 100s of nm scale, respectively.[21−23] Here, we show that ESEM and STXM/NEXAFS, coupled with an RH controlled in situ cell, can be used to measure LLPS in particles with diameter ≅1 μm and less at high spatial resolution. With ESEM, deliquescence and efflorescence phase transitions are readily observed and LLPS can be observed in particles at lower RH when the difference in electron transparencies between the two phases is sufficiently high. Complementary analysis with chemical imaging by STXM/NEXAFS can spatially resolve the organic and inorganic components revealing the potential presence of separate phases even at high RH. These techniques provide information on the composition and morphology of phase separated particles and are well suited for the analysis of LLPS in particles collected directly from the atmosphere.

2. EXPERIMENTAL SECTION

The detailed experimental procedure is provided in the Supporting Information. Briefly, particles were generated from mixed aqueous solutions of limonene secondary organic carbon (LSOC); α, 4-dihydroxy-3-methoxybenzeneaceticacid (HMMA); and polyethylene glycol 400 (PEG-400) with ammonium sulfate (AS) at different mass ratios listed in Table 1. LSOC was generated by dry ozonolysis of D-limonene in a Teflon chamber.[24] All materials were purchased from Sigma-Aldrich with >98% purities. Particles were nebulized from solutions, passed through a diffusion dryer, and collected onto prearranged substrates on the seventh stage (D_{50} = 0.56 μm) of a Multi-Orifice Uniform Deposition Impactor (MOUDI; model 110-R, MSP, Inc.). Samples were collected onto grid-supported carbon-filmed grids (Copper 400 mesh grids coated with Carbon Type-B films, Ted Pella, Inc.) and silicon nitride windows (100 nm thickness SiN_x windows, Silson Ltd.). Sample loading on the substrates was kept low to decrease the amount of particles that ended up coalescing as they grew in size with increasing RH. The detector used for the ESEM imaging was a scanning transmission electron detector.[21] ESEM experiments were done at 275−278 K and STXM/NEXAFS at 300 K. The uncertainty in RH measurements for the ESEM and STXM/NEXAFS experiments is ±2% RH. The in situ cell used for RH control in the STXM/NEXAFS experiments is described in detail in Kelly et al.[25] For all experiments, the RH was raised past the deliquescence point and images were collected during the descent in RH upon drying (or dehydration). The RH values of the observed phase transitions were measured with ESEM. STXM/NEXAFS experiments were subsequently done on the same particle types at RH values above (for deliquescence) and below (for LLPS and efflorescence) the measured transition RH values to further investigate the composition of the phases and the morphology of the particles. For both techniques, beam damage was minimized by using fast scans and selecting new particles for each image/data set.

For the STXM/NEXAFS experiments pixels were 40 nm. Pixels within detected particles were assigned an intensity value (I), particle-free pixels were assigned a background intensity value (I_0), and the optical density (OD) of impacted particles at varying RH values was calculated via the equation:

$$\mathrm{OD} = -\ln(I/I_0) = \mu\rho t \tag{1}$$

where μ is the mass absorption coefficient (cm^2/g), ρ is the density (g/cm^3), and t is the thickness of the particle (cm). Data was collected at the carbon K-edge and the thicknesses of the inorganic (t_{in}) and organic components (t_{org}) were calculated using the OD at the pre-edge (278 eV) and post edge (320 eV):

$$t_{in} = \frac{OD_{278} - \mu_{org,278}\rho_{org}t_{org}}{\mu_{in,278}\rho_{in}} \tag{2}$$

$$t_{org} = \frac{OD_{320} - ((\mu_{in,320}/\mu_{in,278})\mathrm{OD}_{278})}{(\mu_{org,320} - (\mu_{in,320} \times \mu_{org,278}/\mu_{in,278}))\rho_{org}} \tag{3}$$

The mass absorption coefficients for both inorganic and organic components were calculated using the chemical composition of the components (Supporting Information Table S1).[26] For the aqueous systems, the density of water (1.0 g/cm^3) was used for both the inorganic and the organic components of particles. For the effloresced particles, densities of 1.3 g/cm^3 (LSOC), 1.44 g/cm^3 (HMMA), and 1.77 g/cm^3 (AS) were used. Radial scans were used to calculate the average OD at 278 and 320 eV as a function of the distance from the center of the particle. These average OD values were separated into ten bins for each particle and the thickness of the organic and inorganic components in each bin was calculated using eqs

DOI: 10.1021/acs.est.5b00062
Environ. Sci. Technol. 2015, 49, 4995−5002

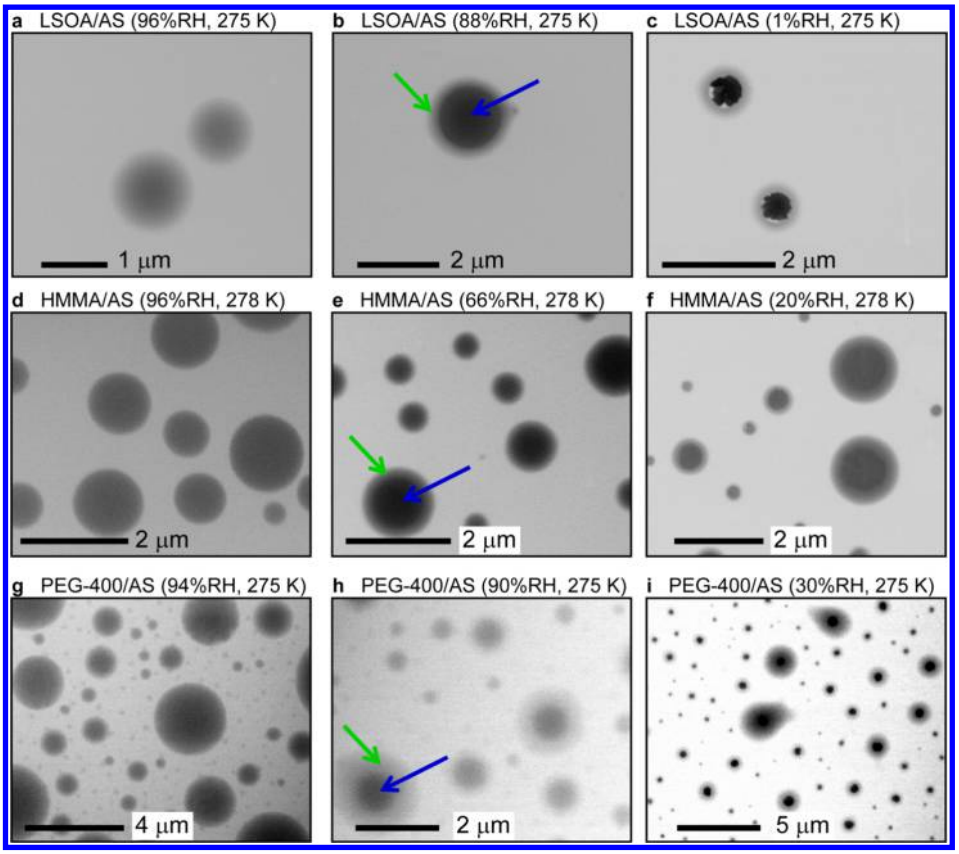

Figure 1. ESEM images of organic/ammonium sulfate (AS) particles at different RH values. (a-c) LSOC/AS with 8:1 organic to inorganic ratio (OIR), (d-f) HMMA/AS 1:1 OIR, (g-i) PEG-400/AS 8:1 OIR. Scale bars for each figure are given in the lower left corner. Blue and green arrows highlight the two phases in the figures with LLPS.

2 and 3. The thickness here refers to the total height of the organic and inorganic components in each bin.

3. RESULTS AND DISCUSSION

3.1. Environmental Scanning Electron Microscopy. Figure 1 shows typical ESEM images taken at decreasing RH from ∼96% to ∼1% for organic/ammonium sulfate particles. Figure 1(a−c) shows LSOC/AS 8:1 organic to inorganic mass ratio (OIR), (d−f) shows HMMA/AS 1:1 OIR, and (g−i) shows PEG-400/AS 8:1 OIR. Darker regions are characteristic of areas with higher atomic number elements and/or a thicker sample region.[21] Particles that are not perfectly circular (Figure 1b and 1i) are likely two particles that were impacted near enough together to coalesce as the particles grew at high RH. The first column shows particles above their deliquescence relative humidity (DRH). The deliquesced particles in Figure 1a (LSOC/AS 8:1 OIR) have a weak radial gradient compared to the more smooth, uniform particles in Figure 1d and 1g. This gradient could result from either incomplete mixing or a slightly different morphology. The far right column shows particles below the efflorescence relative humidity (ERH) of the AS. All of the particles have a smooth outer organic ring surrounding a darker inorganic center with sharp edges. In both the HMMA/AS and PEG/AS samples, the organic appears to completely fill in regions around the crystalline ammonium sulfate center (Figure 1f and 1i). In contrast, the particles in the LSOC/AS sample (Figure 1c) appear to have some brighter white regions which may be "holes" containing little ammonium sulfate or organic matter. These differences are likely caused by different morphologies due to the evaporation process.

At RH values near the separation RH (SRH) the particles show two separate liquid phases, a darker inner phase and a lighter outer phase (Figure 1b, e, and h). The green and blue arrows highlight these two phases. For LSOC/AS 8:1 OIR and PEG-400/AS 8:1 OIR the transition between the inorganic inner phase and organic outer phase is unambiguous. In contrast, HMMA/AS 1:1 OIR has a less apparent radial gradient from the center out to the edge of the particles. Part of the decreased contrast for the HMMA/AS particles is due to the fact that the organic fraction is lower in those particles (1:1) than in the LSOC/AS and PEG-400/AS samples (both 8:1 OIR).

The O/C values of the organics (HMMA 0.63, LSOC ∼0.4,[24] and PEG-400−0.55) all lie within the range (O/C < 0.8) reported for organic compounds that can form two liquid phases with ammonium sulfate.[11,12] The observed deliquescence, efflorescence, and LLPS RH's for all samples from ESEM experiments are listed in Table 1. The LLPS observed for PEG-400 is consistent with results for larger particles (greater than 20 μm) of the same OIR which also showed LLPS at RH ≈ 88.7%, and with bulk measurements.[4,14] The results for the HMMA/AS 1:1 particle are also consistent with previous optical measurements showing LLPS at 81.3 ± 2.5%.[12] These experiments are the first evidence for LLPS in LSOC/AS.

The ESEM experiments were done at 275−278 K, a lower temperature than the STXM experiments and previous optical measurements.[12,14] The ERH of AS particles has no temperature dependence in this temperature range[27] and the DRH of

DOI: 10.1021/acs.est.5b00062
Environ. Sci. Technol. 2015, 49, 4995−5002

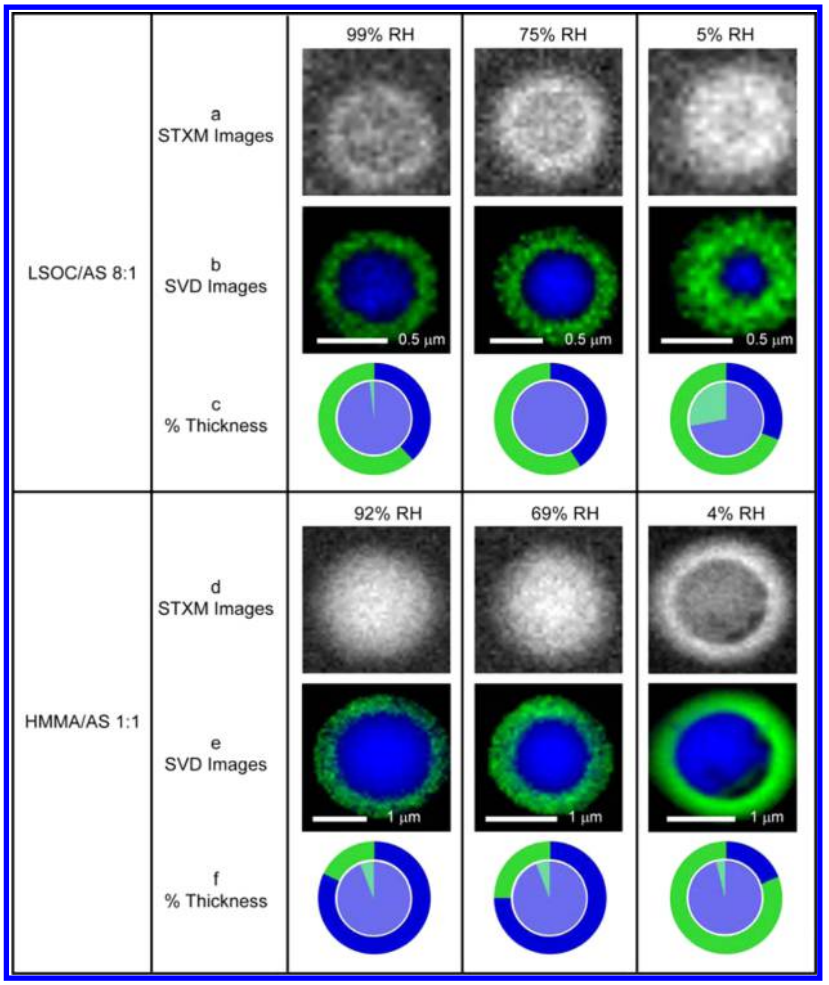

Figure 2. STXM data for LSOC/AS 8:1 OIR (a-c) and HMMA 1:1 OIR (d-f) at high RH (left column), intermediate RH (middle column) and low RH (right column). STXM images at 288.5 eV (a and d). Singular value decomposition images with inorganic (blue) and organic (green) regions (b and e). Fraction of thickness due to organic (green) and inorganic (blue) (c and f). The inner circle (lighter colors) corresponds to the organic versus inorganic fractions in the center of the particles and the outer circle (darker colors) corresponds to the fractions of organic and inorganic components in the particle edge.

AS has a small decrease with increasing temperatures, however, all values were within the uncertainty of the measurement.[28] The lower temperature in the ESEM experiments may increase the viscosity of the organic phase which could impact the RH of the phase transitions. However, very little change in the RH of LLPS has been observed in mixed organic/AS particles between 275 and 290 K[29] and the RH of the transitions observed with ESEM were comparable to available previous optical measurements (Table 1).

The transitions from uniform particles (left most column) to particles with a gradient between a darker inner phase and a lighter outer phase (center column) indicate that ESEM can probe LLPS events in micrometer and submicrometer sized particles. With ESEM, LLPS is apparent when the contrast between the electron transparencies of the two phases is sufficiently large. This difference is easier to see in particles with larger organic fractions and in particles at lower RH which are smaller and have the organic phase distributed over a smaller area. Additional insight into the composition, morphology, and presence of LLPS at higher RH values can be gained with the complementary chemical imaging of STXM/NEXAFS.

3.2. STXM/NEXAFS with in Situ RH Control. *3.2.1. Phase Separation and Phase Compositions.* Two separate liquid phases were observed with STXM/NEXAFS analysis at all measured relative humidity values above the deliquescence point and down to the efflorescence point for both LSOC/AS 8:1 and HMMA/AS 1:1 OIR. Figure 2 shows data from STXM/NEXAFS at the carbon *K*-edge for LSOC/AS 8:1 (a–c) and for HMMA/AS 1:1 OIR (d–f). Every image is a different particle; particles above the deliquescence point are in the first column, particles below the efflorescence point are in the last column, and particles slightly below the LLPS RH observed with ESEM (Table 1) are in the middle column. The top gray figures of each group (Figure 2a and d) are STXM images at 288.5 eV, which is a characteristic energy of the C 1s $\rightarrow \pi^*$ transition for carboxyl groups.[23] The brighter areas in the particles correlate to areas with higher organic content. The set of figures directly below (Figures 2b and e) are singular value decomposition maps of the particles. Pixels colored green have spectra similar to the organic reference spectra and pixels colored blue have spectra similar to the inorganic reference spectra. The reference spectra are from the edge (organic dominated) and center (inorganic dominated) of an effloresced particle (Supporting Information Figure S1).

From the STXM data, all of the particles in the LSOC/AS and HMMA/AS samples had an inorganic inner phase and an organic outer phase at all relative humidity values (Figure 2b and e), even at very high RH conditions above the LLPS RH

DOI: 10.1021/acs.est.5b00062
Environ. Sci. Technol. 2015, 49, 4995–5002

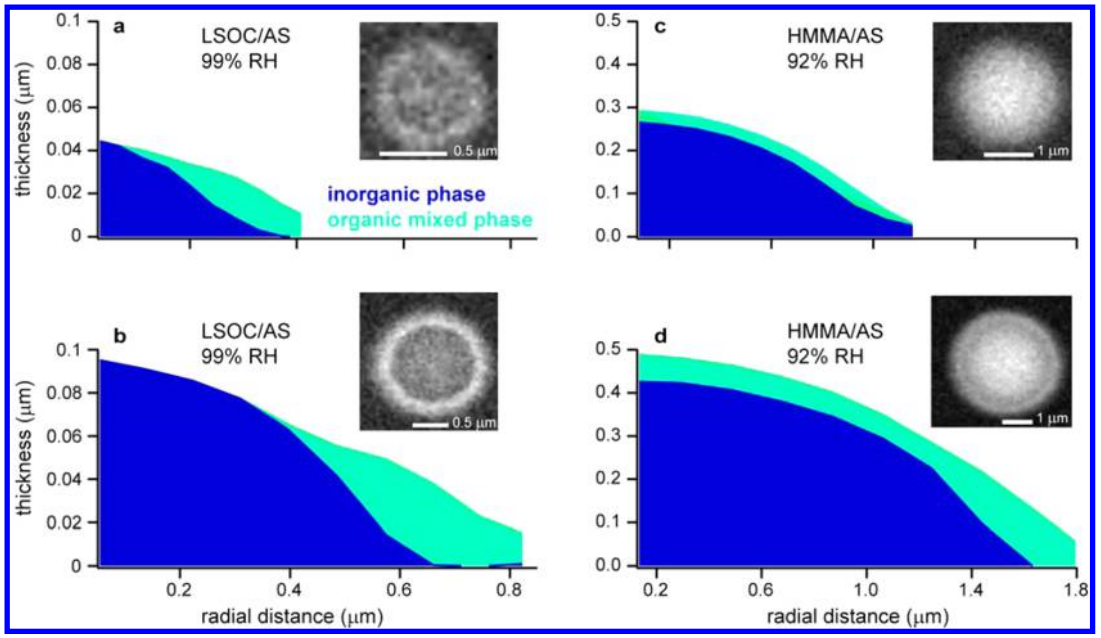

Figure 3. Thickness maps for a mixed organic/inorganic phase (cyan) and a pure AS inorganic phase (blue) from radial scans for two different sized LSOC/AS 8:1 OIR particles at 99% RH (a, b) and two different sized HMMA/AS 1:1 OIR particles at 92% RH (c, d). The organic mixed phase is overlaid on top of the inorganic phase. Insets show STXM images for each particle taken at 288.5 eV.

determined by ESEM. The STXM images suggest the RH of LLPS for HMMA/AS particles with sizes ∼1 μm is higher than the RH values reported so far in the literature for HMMA/AS (Table 1). The STXM images (Figure 2a,b and d,e) indicate a concentration gradient across the radial dimension of the particles which is likely easier to observe in the micrometer-sized particles due to their larger surface area to volume ratio compared to the bulk/larger droplets. The SVD images (Figure 2b and e) show that the concentration gradient has a relatively clear boundary, and we thus identify these as two separate phases. At higher RH conditions during the ESEM experiments, the electron transparencies of the two phases are not substantially different to provide enough contrast for ESEM imaging. Thus, LLPS is observed at lower RH with ESEM. Compared to ESEM and optical microscopy, spectromicroscopy techniques with chemical sensitivity, such as STXM/NEXAFS, are uniquely suited to differentiate the two aqueous phases at RH values above the SRH determined with ESEM and optical microscopy (Table 1).

Figure 2c and f show estimates of the percent thickness of inorganic (blue) and organic (green) in the outer phase (outer, darker circle) and inner phase (inner, lighter circle) for each particle. Radial scans for each particle were generated and each scan was divided into ten bins. The average ratio of organic: inorganic in the first three bins (inner phase) and the last three bins (outer phase) were used to calculate the percent thickness. The uncertainty in these thickness fractions is estimated to be around 5% (see Supporting Information for details). For all particles, the inner phase was dominated by ammonium sulfate. However, all of the particles had an absorption peak at 288.5 eV in all pixels of the particle, indicating the presence of organic. The organic in the center of the particles can be either in an organic phase that coats the particle, mixed in with the inorganic in the inner phase, or a combination of these two.

In the LSOC/AS 8:1 OIR particles above the efflorescence point (Figure 2c, left and middle column) the outer phase was dominated by organic components but still had ∼40% of the thickness as inorganic material. In contrast, the outer phase in the HMMA/AS 1:1 OIR particles above the efflorescence point (Figure 2f, left and middle column) had ∼70−80% of the thickness as inorganic material and only 20−30% of the thickness as organic constituents. The inorganic in these outer phases could be located underneath an organic coating, as unresolved aqueous AS inclusions,[14] and/or mixed in with the aqueous organic component.

For both samples, very little change in composition was observed between similarly sized particles at RH values above the deliquescence point (Figure 2, left column) and particles just below the RH of LLPS (Figure 2, middle column). Upon efflorescence, the mass fraction of AS in the outer phase decreased for both samples (Figure 2, right column). This is consistent with the AS forming a crystalline phase in the center of the particle with an organic dominated outer phase. The small amount of inorganic remaining in the organic outer phase is likely small AS crystals that are either located in the outer phase or that are attached to the center crystal but underneath an organic coating.

3.2.2. Morphology and Size Effects. Figure 3 shows thickness maps of the inorganic (blue) and the mixed organic/inorganic phase (cyan) for two different sized LSOC/AS (a, b) and HMMA/AS (c, d) particles (water thickness not included). In particles with two immiscible phases, the lowest surface energy is reached when the liquid with the lower surface tension is on the surface.[30] The surface tension of the aqueous phase can be lowered when mixed with surfactants. However, here the phase with the lowest surface tension is expected to be the organic phase.[30] The composition of the mixed organic/inorganic phase was calculated using the percent thickness of organic to inorganic at the outer edge of the particle, which for LSOC/AS was 65% organic to 35% inorganic (Supporting InformationFigure S2). If the particles are core−shell, the X-rays would always be traveling through an unknown thickness of coating and, thus, the composition of the core could not be determined. For the thickness maps the

DOI: 10.1021/acs.est.5b00062
Environ. Sci. Technol. 2015, 49, 4995−5002

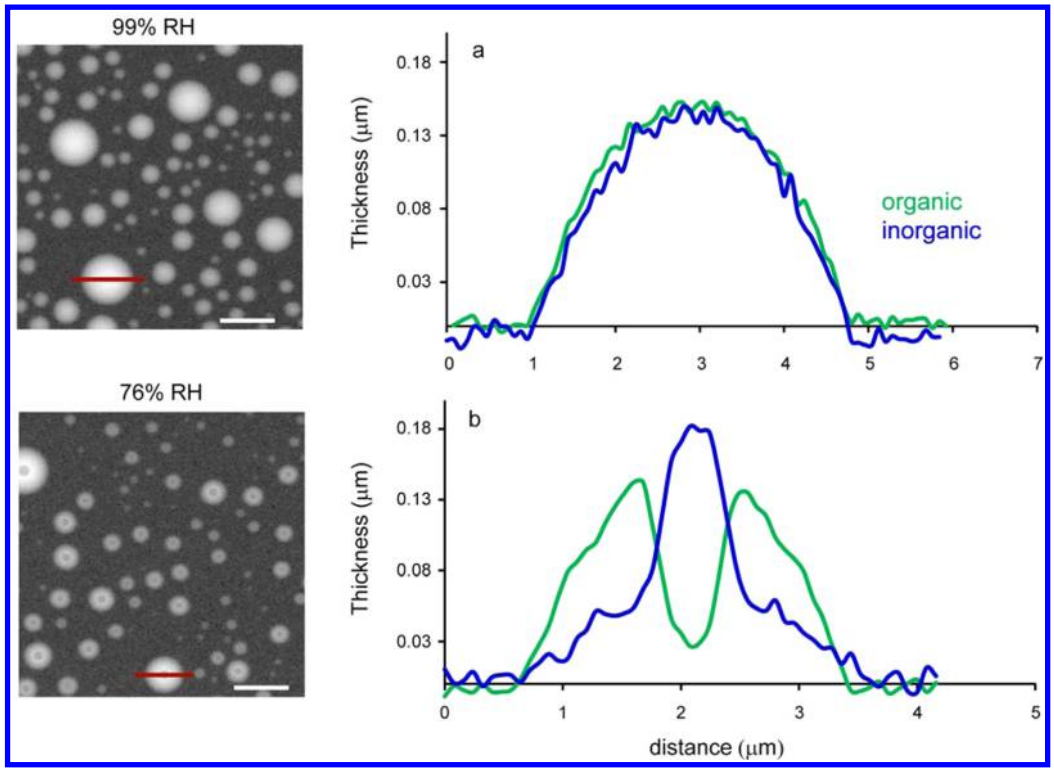

Figure 4. STXM images at 320 eV and compositions for PEG-400/AS 8:1 OIR at (a) 99% RH and (b) 76% RH. The white scale bars in the lower right corner of each image are 4 μm. Particle composition along the linescans, indicated by the red horizontal lines in the left, are shown in the right panels.

inorganic phase was assumed to be pure (100%); organic content in this phase would decrease the calculated thickness of the mixed organic layer.

In Figure 3a and b, LSOC/AS particles display an inorganic dominant inner phase and a mixed organic/inorganic outer phase; the mixed organic outer phase is thicker around the base of the inner phase, extending onto the substrate. The larger particle with a diameter of around 2 μm displayed a distinct organic ring (Figure 3b). The thicker calculated organic layer of this particle is consistent with a morphology where most of the organic phase has flowed down off the center of the particle forming a ring. This organic ring around the edge is consistent with ESEM results, which also showed a clear outer ring in the phase-separated particles. Since the relative thickness of the two phases has an estimated uncertainty of around 5% and the composition of the center inorganic phase cannot be determined (see previous paragraph) the morphology can be either core−shell with a very thin mixed organic coating or partially engulfed with the central inorganic phase exposed to the gas phase.

Thickness maps for HMMA/AS 1:1 OIR indicate a different morphology; the outer phase is a roughly uniform coating over the entire particle for both small and large particles (Figure 3c and d). Since the organic fraction is lower in these particles, the composition of the mixed organic phase was calculated based on the composition at the outer edge of the larger particle, which was about 50:50 (Supporting Information Figure S3). The difference in morphology can also be seen in the STXM images where a larger contrast between the inner phase and outer phase is observed in the LSOC/AS particles (Figure 3a and b) compared to the HMMA/AS particles (Figure 3c and d). A thin, fairly uniform coating for HMMA/AS particles is consistent with the smaller changes observed with ESEM with decreasing RH; the transmitted electrons would pass through similar composition throughout the particle and any outer organic ring would be very thin and therefore hardly detectable.

The difference in morphology suggests differences in the physical characteristics of the two different organic solutions. The lack of a uniform thickness for the LSOC/AS particles on the substrate may in part be driven by interactions of the mixed organic phase with the inorganic phase or with the substrate. It also suggests that the aqueous organic phase in liquid−liquid phase-separated particles with characteristics similar to that of LSOC could potentially form partially engulfed structures in airborne particles.[30] However, work with levitated droplets[5,30] and/or impacted aerosols after cycling[18,19] are needed to understand the effect of the substrate on the observed morphologies for these particles.

Organic coatings on aqueous particles have been observed to decrease the reactive uptake of N_2O_5.[31,32] The solubility, the diffusion rate through the organic phase, and the reaction rate constant for N_2O_5 can all depend upon the composition and thickness of an outer organic phase in a particle with core−shell morphology. Thus, chemical imaging techniques such as STXM/NEXFS and ESEM, which can provide insights into the composition of the outer phase as well as some information on the morphology of impacted ambient aerosol particles, are powerful tools for the investigation of the impacts of LLPS on atmospheric chemistry.

3.2.3. PEG-400/AS. STXM/NEXAFS analysis of phase transitions in PEG 400/AS 8:1 OIR showed fully mixed particles at high RH and phase-separated particles at intermediate RH. The presence of a completely mixed particle at high RH as well as the RH values observed for phase transitions were very similar to previous observations for particles of the same composition.[14] Figure 4 shows STXM

DOI: 10.1021/acs.est.5b00062
Environ. Sci. Technol. 2015, 49, 4995−5002

images on the left and thickness maps from linescans across representative particles at high RH (a) and intermediate RH (b). At high RH, the particle has a uniform thickness of organic and inorganic components. At intermediate RH, the particle has two phases: a central phase that is dominated by inorganic and an outer phase that is dominated by organic. The outer phase has a composition (by thickness) of ~70% PEG-400 and ~30% AS. In contrast, the center of the particle has a composition (by thickness) of ~10% PEG-400 and ~90% AS (Supporting Information Figure S4). There is a large amount of organic in these particles, which resulted in donut like images in STXM (Figure 4b) where the brightest regions (where the organic is thickest) surround the inner phase, which has a low organic content. The morphology observed here for the phase separated particles is similar to the half sphere in a spherical calotte structure proposed by Ciobanu et al.[14]

LLPS events were observed in micrometer-sized impacted LSOC/AS, HMMA/AS, and PEG-400/AS particles using the complementary spectromicroscopic techniques of ESEM and STXM/NEXAFS. The inhomogeneity at high RH observed with STXM for both HMMA/AS and LSOC/AS particles indicates that ESEM and optical methods show LLPS only when the difference in optical properties of the two phases is sufficiently high; chemical imaging techniques are necessary to investigate LLPS events at higher RH. Thus, ESEM provides measurements of DRH, ERH, and the RH at which LLPS is optically visible. Subsequent analysis by STXM/NEXAFS, in combination with an RH controlled in situ cell, provides further information on the composition of the phases, the morphology of the particles, and on the extent of mixing at high RH. These sample cases demonstrate that spectromicroscopic in situ techniques can be used to provide details on phase transitions and on the composition of the surface of impacted ambient aerosols throughout hygroscopic cycles.

■ ASSOCIATED CONTENT

Ⓢ Supporting Information

Supporting Information provides detailed experimental procedures including sample preparation, phase separation measurements with ESEM and STXM/NEXAFS, organic and inorganic thickness calculations, and STXM spectral analysis. Table S1 provides mass absorption coefficients used in the thickness calculations, Figure S1 provides spectra used for singular value decomposition, and Figure S2 −S4 provide the thickness percentage of organic to inorganic for the particles shown in Figures 3 and 4 of the main text. This material is available free of charge via the Internet at http://pubs.acs.org.

■ AUTHOR INFORMATION

Corresponding Author

*Phone: 510-495-2775; fax: 510-495-2690; e-mail: MKGilles@lbl.gov.

Present Addresses

[#]Department of Civil and Environmental Engineering, Massachusetts Institute of Technology, Cambridge, Massachusetts 02139, United States.

[▽]Carl Zeiss X-ray Microscopy Inc., Pleasanton, California 94588, United States.

[●]Department of Physics and Astronomy, University of Würzburg, 97070 Würzburg, Germany.

Notes

The authors declare no competing financial interest.

■ ACKNOWLEDGMENTS

STXM/NEXAFS was done at beamlines 5.3.2.2 and 11.0.2 at The Advanced Light Source (ALS) at Lawrence Berkeley National Laboratory (LBNL) supported by the Director, Office of Science, Office of Basic Energy Sciences, (beamline 11.0.2 is also supported by the Division of Chemical Sciences, Geosciences, and Biosciences) of the U.S. Department of Energy under Contract No. DE-AC02-05CH11231. In-situ phase separation experiments at beamline 11.0.2 and analysis were supported by the Condensed Phase and Interfacial Molecular Sciences program under the same Contract No. Dry characterization of the samples at beamline 5.3.2.2 and analysis was supported by the U.S. Department of Energy's Atmospheric System Research, an Office of Science, Office of Biological and Environmental Research program (BER ASR). We acknowledge the continued support of ALS scientists A.L.D Kilcoyne and Tolek Tyliszczak. N.L. acknowledges the student exchange program between the University of Würzburg and U.C. Berkeley (curator Professor C. Gould, Würzburg. S.R.L. acknowledges additional support from the Office of Assistant Secretary of Defense for Research and Engineering, National Security Science and Engineering Faculty Fellowship. A.L. and B.W. acknowledge support from the Chemical Imaging Initiative of the Laboratory Directed Research and Development program at Pacific Northwest National Laboratory (PNNL). ESEM imaging of particles was performed at the Environmental Molecular Sciences Laboratory, a national scientific user facility sponsored by OBER at Pacific Northwest National Laboratory. PNNL is operated by the U.S. Department of Energy by Battelle Memorial Institute under contract DE-AC06-76RL0.

■ REFERENCES

(1) Martin, S. T.; Rosenoern, T.; Chen, Q.; Collins, D. R. Phase changes of ambient particles in the Southern Great Plains of Oklahoma. *Geophys. Res. Lett.* **2008**, *35*, L22801 DOI: 10.1029/2008GL035650.

(2) You, Y.; Renbaum-Wolff, L.; Carreras-Sospedra, M.; Hanna, S. J.; Hiranuma, N.; Kamal, S.; Smith, M. L.; Zhang, X. L.; Weber, R. J.; Shilling, J. E.; Dabdub, D.; Martin, S. T.; Bertram, A. K. Images reveal that atmospheric particles can undergo liquid-liquid phase separations. *Proc. Natl. Acad. Sci. U. S. A.* **2012**, *109* (33), 13188−13193.

(3) You, Y.; Smith, M. L.; Song, M. J.; Martin, S. T.; Bertram, A. K. Liquid-liquid phase separation in atmospherically relevant particles consisting of organic species and inorganic salts. *Int. Rev. Phys. Chem.* **2014**, *33* (1), 43−77.

(4) Marcolli, C.; Krieger, U. K. Phase changes during hygroscopic cycles of mixed organic/inorganic model systems of tropospheric aerosols. *J. Phys. Chem. A* **2006**, *110* (5), 1881−1893.

(5) Song, M. J.; Marcolli, C.; Krieger, U. K.; Lienhard, D. M.; Peter, T. Morphologies of mixed organic/inorganic/aqueous aerosol droplets. *Faraday Discuss.* **2013**, *165*, 289−316.

(6) Kwamena, N. O. A.; Buajarern, J.; Reid, J. P. Equilibrium Morphology of Mixed Organic/Inorganic/Aqueous Aerosol Droplets: Investigating the Effect of Relative Humidity and Surfactants. *J. Phys. Chem. A* **2010**, *114* (18), 5787−5795.

(7) Petters, M. D.; Kreidenweis, S. M. A single parameter representation of hygroscopic growth and cloud condensation nucleus activity. *Atmos. Chem. Phys.* **2007**, *7* (8), 1961−1971.

(8) Cosman, L. M.; Knopf, D. A.; Bertram, A. K. N2O5 reactive uptake on aqueous sulfuric acid solutions coated with branched and straight-chain insoluble organic surfactants. *J. Phys. Chem. A* **2008**, *112* (11), 2386−2396.

DOI: 10.1021/acs.est.5b00062
Environ. Sci. Technol. 2015, 49, 4995−5002

(9) Zuend, A.; Seinfeld, J. H. Modeling the gas-particle partitioning of secondary organic aerosol: The importance of liquid-liquid phase separation. *Atmos. Chem. Phys.* **2012**, *12* (9), 3857−3882.
(10) Fuzzi, S.; Andreae, M. O.; Huebert, B. J.; Kulmala, M.; Bond, T. C.; Boy, M.; Doherty, S. J.; Guenther, A.; Kanakidou, M.; Kawamura, K.; Kerminen, V. M.; Lohmann, U.; Russell, L. M.; Poschl, U. Critical assessment of the current state of scientific knowledge, terminology, and research needs concerning the role of organic aerosols in the atmosphere, climate, and global change. *Atmos. Chem. Phys.* **2006**, *6*, 2017−2038.
(11) Song, M.; Marcolli, C.; Krieger, U. K.; Zuend, A.; Peter, T. Liquid-liquid phase separation in aerosol particles: Dependence on O:C, organic functionalities, and compositional complexity. *Geophys. Res. Lett.* **2012**, *39*, L19801 DOI: 10.1029/2012GL052807.
(12) You, Y.; Renbaum-Wolff, L.; Bertram, A. K. Liquid-liquid phase separation in particles containing organics mixed with ammonium sulfate, ammonium bisulfate, ammonium nitrate or sodium chloride. *Atmos. Chem. Phys.* **2013**, *13* (23), 11723−11734.
(13) Bertram, A. K.; Martin, S. T.; Hanna, S. J.; Smith, M. L.; Bodsworth, A.; Chen, Q.; Kuwata, M.; Liu, A.; You, Y.; Zorn, S. R. Predicting the relative humidities of liquid-liquid phase separation, efflorescence, and deliquescence of mixed particles of ammonium sulfate, organic material, and water using the organic-to-sulfate mass ratio of the particle and the oxygen-to-carbon elemental ratio of the organic component. *Atmos. Chem. Phys.* **2011**, *11* (21), 10995−11006.
(14) Ciobanu, V. G.; Marcolli, C.; Krieger, U. K.; Weers, U.; Peter, T. Liquid-liquid phase separation in mixed organic/inorganic aerosol particles. *J. Phys. Chem. A* **2009**, *113* (41), 10966−10978.
(15) Song, M.; Marcolli, C.; Krieger, U. K.; Zuend, A.; Peter, T. Liquid-liquid phase separation and morphology of internally mixed dicarboxylic acids/ammonium sulfate/water particles. *Atmos. Chem. Phys.* **2012**, *12* (5), 2691−2712.
(16) Zhou, Q.; Pang, S. F.; Wang, Y.; Ma, J. B.; Zhang, Y. H. Confocal Raman studies of the evolution of the physical state of mixed phthalic acid/ammonium sulfate aerosol droplets and the effect of substrates. *J. Phys. Chem. B* **2014**, *118* (23), 6198−6205.
(17) Brunamonti, S.; Krieger, U. K.; Marcolli, C.; Peter, T., Redistribution of black carbon in aerosol particles undergoing liquid-liquid phase separation. *Geophys. Res. Lett.* **2015**, DOI: 10.1002/2014GL062908.
(18) Veghte, D. P.; Altaf, M. B.; Freedman, M. A. Size dependence of the structure of organic aerosol. *J. Am. Chem. Soc.* **2013**, *135* (43), 16046−16049.
(19) Veghte, D. P.; Bittner, D. R.; Freedman, M. A. Cryo-transmission electron microscopy imaging of the morphology of submicrometer aerosol containing organic acids and ammonium sulfate. *Anal. Chem.* **2014**, *86*, 2436−2442.
(20) Zelenay, V.; Ammann, M.; Krepelova, A.; Birrer, M.; Tzvetkov, G.; Vernooij, M. G. C.; Raabe, J.; Huthwelker, T. Direct observation of water uptake and release in individual submicrometer sized ammonium sulfate and ammonium sulfate/adipic acid particles using X-ray microspectroscopy. *J. Aerosol. Sci.* **2011**, *42* (1), 38−51.
(21) Laskin, A.; Cowin, J. P.; Iedema, M. J. Analysis of individual environmental particles using modern methods of electron microscopy and X-ray microanalysis. *J. Electron Spectrosc. Relat. Phenom.* **2006**, *150* (2−3), 260−274.
(22) Laskin, A.; Wietsma, T. W.; Krueger, B. J.; Grassian, V. H., Heterogeneous chemistry of individual mineral dust particles with nitric acid: A combined CCSEM/EDX, ESEM, and ICP-MS study. *J. Geophys. Res.: Atmos.* **2005**, *110* (D10); DOI: 10.1029/2004JD005206.
(23) Moffet, R. C.; Tivanski, A. V.; Gilles, M. K., Scanning transmission X-ray microscopy applications in atmospheric aerosol research. In *Fundamentals and Applications in Aerosol Spectroscopy*; Signorell, R., Reid, J. P., Eds.; CRC Press, Taylor & Francis Group: Boca Raton, Fl, 2011; pp 434−436.
(24) Bateman, A. P.; Nizkorodov, S. A.; Laskin, J.; Laskin, A. Time-resolved molecular characterization of limonene/ozone aerosol using high-resolution electrospray ionization mass spectrometry. *Phys. Chem. Chem. Phys.* **2009**, *11* (36), 7931−7942.
(25) Kelly, S. T.; Nigge, P.; Prakash, S.; Laskin, A.; Wang, B. B.; Tyliszczak, T.; Leone, S. R.; Gilles, M. K. An environmental sample chamber for reliable scanning transmission X-ray microscopy measurements under water vapor. *Rev. Sci. Instrum.* **2013**, *84* (7), 073708 DOI: 10.1063/1.4816649.
(26) Henke, B. L.; Gullikson, E. M.; Davis, J. C. X-ray interactions—Photoabsorption, scattering, transmission at reflection at E = 50−30,000 EV, Z = 1−92 (vol 54, pg 181, 1993). *Atom. Data Nucl. Data Tables* **1993**, *55* (2), 349−349.
(27) Bodsworth, A.; Zobrist, B.; Bertram, A. K. Inhibition of efflorescence in mixed organic-inorganic particles at temperatures less than 250 K. *Phys. Chem. Chem. Phys.* **2010**, *12* (38), 12259−12266.
(28) Parsons, M. T.; Mak, J.; Lipetz, S. R.; Bertram, A. K., Deliquescence of malonic, succinic, glutaric, and adipic acid particles. *J. Geophys. Res.* **2004**, *109* (D6); DOI 10.1029/2003JD004075.
(29) You, Y.; Bertram, A. K. Effects of molecular weight and temperature on liquid-liquid phase separation in particles containing organic species and ammonium sulfate. *Atmos. Chem. Phys.* **2015**, *15*, 1351−1365 DOI: 10.5194/acp-15-1351-2015.
(30) Reid, J. P.; Dennis-Smither, B. J.; Kwamena, N. O. A.; Miles, R. E. H.; Hanford, K. L.; Homer, C. J. The morphology of aerosol particles consisting of hydrophobic and hydrophilic phases: Hydrocarbons, alcohols and fatty acids as the hydrophobic component. *Phys. Chem. Chem. Phys.* **2011**, *13* (34), 15559−15572.
(31) Anttila, T.; Kiendler-Scharr, A.; Tillmann, R.; Mentel, T. F. On the reactive uptake of gaseous compounds by organic-coated aqueous aerosols: Theoretical analysis and application to the heterogeneous hydrolysis of N_2O_5. *J. Phys. Chem. A* **2006**, *110* (35), 10435−10443.
(32) Folkers, M.; Mentel, T. F.; Wahner, A. Influence of an organic coating on the reactivity of aqueous aerosols probed by the heterogeneous hydrolysis of N_2O_5. *Geophys. Res. Lett.* **2003**, *30* (12), 1644 DOI: 10.1029/2003GL017168.

DOI: 10.1021/acs.est.5b00062
Environ. Sci. Technol. 2015, 49, 4995−5002